Computers and Structures 126 (2013) 15–28

Contents lists available at SciVerse ScienceDirect

Computers and Structures

journal homepage: www.elsevier.com/locate/compstruc

Component mode synthesis techniques for finite element model updating

Costas Papadimitriou *, Dimitra-Christina Papadioti

University of Thessaly, Department of Mechanical Engineering, Volos 38334, Greece

ARTICLE INFO

Article history:
Received 3 July 2012
Accepted 17 October 2012
Available online 17 November 2012

Keywords:
Model updating
Structural identification
Multi-objective optimization
Bayesian inference
Transitional MCMC
Component mode synthesis

ABSTRACT

Deterministic and Bayesian finite element (FE) model updating techniques are computationally very demanding operations due to the large number of FE model re-analyses required. Component mode synthesis techniques are proposed to carry out the re-analyses efficiently in a substantially reduced space of generalized coordinates using exact component modes and characteristic interface modes computed only once from a reference FE model. The re-assembling of the reduced-order system matrices from components and interface modes is avoided. Theoretical and computational developments are demonstrated with model updating and damage identification applications for a highway bridge using a high fidelity model and simulated measurements.

1. Introduction

Structural model updating methods (e.g. [1–3]) are used to reconcile mathematical models, usually discretized finite element (FE) models, with experimental data. Structural model parameter estimation problems based on identified modal characteristics (modal frequencies and mode shapes), are often formulated as weighted least-squares problems (e.g. [2,4–8]) in which metrics, measuring the residuals between measured and model predicted modal characteristics, are build up into a single weighted residuals metric formed as a weighted average of the multiple individual metrics using weighting factors. Standard optimization techniques are then used to find the optimal values of the structural parameters that minimize the single weighted residuals metric. Due to model error and measurement noise, the results of the optimization are affected by the values assumed for the weighting factors. The model updating problem has also been formulated as a multi-objective optimization problem [9,10] that allows the simultaneous minimization of the multiple metrics, eliminating the need for using arbitrary weighting factors for weighting the relative importance of each metric in the overall measure of fit. The multi-objective parameter estimation methodology provides multiple Pareto optimal structural models in the sense that the fit each Pareto optimal model provides in a group of measured modal properties cannot be improved without deteriorating the fit in at least one other modal group. The Normal Boundary Intersection algorithm [11] is used to compute the Pareto optimal solutions.

Bayesian techniques [12,13] have also been proposed to quantify the uncertainty in the parameters of a FE model, select the best model class from a family of competitive model classes [14,15], as well as propagate uncertainties for robust response and reliability predictions [16]. Posterior probability density functions (PDFs) are derived that quantify the uncertainty in the model parameters based on the data. These PDFs are formulated in terms of the modal residuals involved in the aforementioned single and multi objectives deterministic methods. The Bayesian tools for identifying uncertainty models as well as performing robust prediction analyses are Laplace methods of asymptotic approximation and more accurate stochastic simulation algorithms (SSA) such as Markov Chain Monte Carlo (MCMC) [17], Transitional MCMC [18] and Delayed Rejection Adaptive Metropolis [19]. Similar to the deterministic FE model updating techniques, the asymptotic approximations in the Bayesian framework involve solving an optimization problem for finding the most probable model, as well as estimating the Hessian of the logarithm of the posterior PDF at the most probable model for describing the uncertainty in the model parameters. The SSA algorithms involve generating samples for tracing and then populating the important uncertainty region in the parameter space, as well as evaluating integrals over high-dimensional spaces of the uncertain model parameters.

The optimal structural models and their uncertainties resulting from model updating methods can be used for improving the model response and reliability predictions [16,20], for assessing structural health and identifying structural damage [5–8,21–28] and for improving effectiveness of structural control devices [29].

Abbreviations: FE, finite element; DOF, Degrees of Freedom; PDF, probability density function; SSA, stochastic simulation algorithm; MCMC, Markov chain Monte Carlo; TMCMC, Transitional MCMC; CMS, component mode synthesis.

* Corresponding author. Tel.: +30 2421074006; fax: +30 2421074012.
E-mail address: costasp@uth.gr (C. Papadimitriou).

0045-7949/$ - see front matter © 2012 Elsevier Ltd. All rights reserved.
http://dx.doi.org/10.1016/j.compstruc.2012.10.018

The aforementioned optimization and SSA algorithms require a moderate to very large number of FE re-analyses to be performed over the space of model parameters. Consequently, the computational demands depend highly on the number of FE re-analyses and the time required for performing a FE analysis. In addition, gradient-based optimization algorithms require the estimation of the gradients of the residuals which may also add substantially to the computational effort. For high fidelity FE models involving hundreds of thousands or even million DOF, the computational demands may be large or even excessive. The present work proposes efficient methods based on dynamic reduction techniques to alleviate the computational burden involved in the implementation of deterministic and probabilistic (Bayesian) techniques for FE model updating.

Specifically, component mode synthesis (CMS) techniques [30–32] are widely used to carry out system analyses in a significantly reduced space of generalized coordinates. Such techniques have been incorporated in methods for uncertainty management in structural dynamics to efficiently handle the computational effort in system re-analyses that arise from FE model variations caused by variations in the values of the uncertain parameters [33,34]. Such variations in the values of the model parameters require that the computation of the component and/or system modes be repeated in each re-analysis. As a result, a computational overhead arises at component level which may be substantial. The main objective in methods involving re-analyses of models with varying properties is to avoid, to the extent possible, the re-computation of the eigenproperties at the component or system level. Perturbation techniques [35,36] provide accurate results locally for small variations of the model parameters about a reference structure. To improve the accuracy of the approximations for large variation of the model parameters, most efforts have been concentrated in approximating the modes at the component or system level in terms of the modes of a family of structures corresponding to support points in the parameter space [33]. Linear and quadratic interpolations of the structural mass and stiffness matrix and the matrix of eigenvectors at the component and/or system level using support points in the larger region in the parameter space have been proposed in [37]. Such methods have been successfully used for model updating of large-order models of structures [38,39], while similar methods have been developed for damage detection at component level [40]. Such techniques proved to be quite effective in substantially reducing the computational demands in problems requiring system re-analyses.

In this work, a framework is presented for integrating the Craig–Bampton CMS [30,31] technique into existing FE model updating formulations in order to reduce the time consuming operations involved in re-analyses of large-order models of hundreds of thousands or millions degrees of freedom. The proposed method exploits the fact that in FE model parameterization schemes the stiffness matrix of the structure often depends linearly on the parameters of the model and also that a parameter usually represents a global property (e.g. the modulus of elasticity) of a substructure. The division of the structure into components is then guided by the FE parameterization scheme so that the stiffness matrix that arise for each one of the introduced components to depend linearly on only one of the parameters to be estimated. In this case the fixed-interface and constraint modes of the components for any value of the model parameters can be obtained exactly from the fixed-interface and constraint modes corresponding to a single reference FE model, avoiding re-analyses at component level. Additional substantial reductions in computational effort are also proposed by reducing the number of interface DOF using characteristic interface modes through a Ritz coordinate transformation. The repeated solutions of the component and interface eigen-problems are avoided, reducing drastically the computational demands in FE formulations, without compromising the solution accuracy. It is also shown that the linear expansions of the original mass and stiffness matrices in terms of the structural parameters are preserved for the reduced mass and stiffness matrices. Thus, the re-assembling of the reduced system matrices from the original matrices is also avoided in the execution of the system re-analyses. The only time consuming operation left is the re-analysis of the eigenproblem of the reduced-order model. It is finally demonstrated that the new developments are readily accommodated in existing FE model updating formulations and software with minimal modifications.

Deterministic and Bayesian FE model updating formulations along with computational aspects are presented in Section 2. The mathematical background for the Craig-Bampton CMS technique and a technique to reduce the DOF in the interface between components using characteristic interface modes, is outlined in Section 3. The integration of the CMS technique with model updating formulations is given in Section 4. In Section 5 the effectiveness of the proposed algorithms, in terms of computational efficiency and accuracy, is demonstrated with applications on model updating and damage identification of a bridge using simulated data and a high fidelity model with hundreds of thousands of DOF. Conclusions are summarized in Section 6.

2. Finite element model updating using modal characteristics

Consider a parameterized linear FE model class M of a structure and let $\underline{\theta} \in R^{N_\theta}$ be a vector of free structural model parameters to be estimated using a set of modal properties identified from vibration measurements. The identified modal properties consist of the square of the modal frequencies, $\hat{\lambda}_r = \hat{\omega}_r^2$, and the mode shape components $\underline{\hat{\phi}}_r \in \mathbb{R}^{N_0}$ at N_0 measured DOF, for $r = 1,\ldots,m$, where m is the number of observed modes. The values of the parameter vector $\underline{\theta}$ are estimated so that the modal frequencies $\lambda_r(\underline{\theta}) = \omega_r^2(\underline{\theta})$ and modeshapes $\underline{\phi}_r(\underline{\theta}) \in \mathbb{R}^{N_0}$, predicted by the FE model, best matches the experimentally obtained modal data D. For this, the following modal frequency and mode shape residuals

$$J_1(\underline{\theta}) = \sum_{r=1}^{m} \varepsilon_{\lambda_r}^2(\underline{\theta}) = \sum_{r=1}^{m} \frac{\left[\lambda_r(\underline{\theta}) - \hat{\lambda}_r\right]^2}{\hat{\lambda}_r^2} \tag{1}$$

and

$$J_2(\underline{\theta}) = \sum_{r=1}^{m} \varepsilon_{\underline{\phi}_r}^2(\underline{\theta}) = \sum_{r=1}^{m} \frac{\left\| \beta_r(\underline{\theta})\underline{\phi}_r(\underline{\theta}) - \underline{\hat{\phi}}_r \right\|^2}{\|\underline{\hat{\phi}}_r\|^2} = \sum_{r=1}^{m} \left[1 - MAC_r^2(\underline{\theta})\right] \tag{2}$$

are introduced to measure the differences ε_{λ_r} and $\varepsilon_{\underline{\phi}_r}$ for the modal frequencies and mode shape components between the identified modal data and the model predicted modal data, respectively, where $\beta_r(\underline{\theta}) = \underline{\hat{\phi}}_r^T \underline{\phi}_r(\underline{\theta}) / \|\underline{\phi}_r(\underline{\theta})\|^2$ is a normalization constant that guaranties that the measured mode shape $\underline{\hat{\phi}}_r$ at the measured DOF is closest to the model mode shape $\beta_r(\underline{\theta})\underline{\phi}_r(\underline{\theta})$ predicted by the particular value of $\underline{\theta}$ $MAC_r = \underline{\phi}_r^T \underline{\hat{\phi}}_r / (\|\underline{\phi}_r\| \|\underline{\hat{\phi}}_r\|)$ is the modal assurance criterion between the experimentally identified and model predicted mode shapes for the r-th mode, and $\|\underline{z}\|^2 = \underline{z}^T \underline{z}$ is the usual Euclidian norm.

The mode shape components $\underline{\phi}_r(\underline{\theta}) = L\underline{\varphi}_r(\underline{\theta}) \in \mathbb{R}^{N_0}$ at the N_0 measured DOF involved in (2) are computed from the full mode shapes $\underline{\varphi}_r(\underline{\theta}) \in \mathbb{R}^n$ that satisfy the eigenvalue problem

$$[K(\underline{\theta}) - \lambda_r(\underline{\theta}) M(\underline{\theta})]\underline{\varphi}_r(\underline{\theta}) = \underline{0} \tag{3}$$

where $K(\underline{\theta}) \in \mathbb{R}^{n \times n}$ and $M(\underline{\theta}) \in \mathbb{R}^{n \times n}$ are respectively the stiffness and mass matrices of the FE model of the structure, n is the number of model DOF, and $L \in R^{N_0 \times n}$ is an observation matrix, usually

comprised of zeros and ones, that maps the n model DOF to the N_0 observed DOF. For a model with large number of DOF, $N_0 \ll n$.

2.1. Formulation as single- and multi-objective optimization problems

The estimation of the model parameters is traditionally formulated as a minimization of the weighted residuals

$$J(\underline{\theta}; w) = J_1(\underline{\theta}) + wJ_2(\underline{\theta}) \tag{4}$$

where $w \in [0,\infty)$. The results of the identification depend on the weight value used. The parameter estimation problem can also be formulated as a multi-objective optimization problem [9,10] of finding the values of $\underline{\theta}$ that simultaneously minimizes the objectives

$$\underline{J}(\underline{\theta}) = (J_1(\underline{\theta}), J_2(\underline{\theta})) \tag{5}$$

where $\underline{J}(\underline{\theta})$ is the objective vector defined over the two-dimensional objective space. For conflicting objectives $J_1(\underline{\theta})$ and $J_2(\underline{\theta})$, there is no single optimal solution, but rather a set of alternative solutions, known as Pareto optimal solutions, that are optimal in the sense that no other solutions in the parameter space are superior to them when both objectives are considered. The set of objective vectors $\underline{J}(\underline{\theta})$ corresponding to the set of Pareto optimal solutions $\underline{\theta}$ is called Pareto optimal front. The multiple Pareto optimal solutions are due to modeling and measurement errors. The solution obtained by optimizing (4) for any weight value is a Pareto optimal solution [10]. However, in order to adequately describe the Pareto optimal solutions by uniformly spaced points along the solution manifold in the parameter space, the multi-objective optimization problem is preferred since varying the weight value in (4) may miss significant portions of the Pareto optimal solutions in the objective and parameter space.

2.2. Bayesian formulation

Bayesian methods are used to quantify the uncertainty in the FE model parameters as well as select the most probable FE model class among a family of competitive model classes based on the measured modal data. The structural model class M is augmented to include the prediction error model class that postulates zero-mean Gaussian models for the modal frequency and mode shape error terms ε_{λ_r} and ε_{ϕ_r} in (1) and (2), respectively, with equal variances σ^2 for all modal frequency errors ε_{λ_r} and equal variances σ^2/w for all mode shape errors ε_{ϕ_r}. Using PDFs to quantify uncertainty and following the Bayesian formulation (e.g. [5,12,21]), the posterior PDF $p(\underline{\theta},\sigma|D,\mathsf{M})$ of the structural model parameters $\underline{\theta}$ and the prediction error parameter σ given the data D and the model class M can be obtained in the form

$$p(\underline{\theta},\sigma|D,\mathsf{M}) = \frac{[p(D|\mathsf{M})]^{-1}}{\left(\sqrt{2\pi}\sigma\right)^{m(N_0+1)}} \exp\left[-\frac{1}{2\sigma^2}J(\underline{\theta};w)\right] \quad \pi(\underline{\theta},\sigma|\mathsf{M}) \tag{6}$$

where the distribution $\pi(\underline{\theta},\sigma|\mathsf{M})$ is the prior PDF of the structural model parameters $\underline{\theta}$ and the prediction error parameter model σ, and $p(D|\mathsf{M})$ is the evidence of the model class M.

For large enough number of experimental data, and assuming for simplicity a single dominant most probable model, the posterior distribution of the model parameters can be asymptotically approximated by the multi-dimensional Gaussian distribution [12] centered at the most probable value $(\underline{\hat{\theta}},\hat{\sigma})$ of the model parameters that minimizes the function

$$\begin{aligned} g(\underline{\theta},\sigma;\mathsf{M}) &= -\ln p(\underline{\theta},\sigma|D,\mathsf{M}) \\ &= 0.5\sigma^{-2}J(\underline{\theta};w) + 0.5m(N_0+1)\ln\sigma^2 - \ln\pi(\underline{\theta},\sigma|\mathsf{M}) \end{aligned} \tag{7}$$

with covariance equal to the inverse of the Hessian $h(\underline{\theta},\sigma)$ of the function $g(\underline{\theta},\sigma;\mathsf{M})$ evaluated at the most probable value. For a uniform prior distribution, the most probable value of the FE model parameters $\underline{\theta}$ coincides with the estimate obtained by minimizing the weighted residuals in (4). An asymptotic approximation based on Laplace's method is also available to give an estimate of the model evidence $p(D|\mathsf{M})$ in (6) [14,41]. The estimate is also based on the most probable value of the model parameters and the value of the Hessian $h(\underline{\theta},\sigma)$ evaluated at the most probable value.

The Bayesian probabilistic framework is also used to compare two or more competing model classes and select the optimal model class based on the available data. Consider a family $\mathsf{M}_{Fam} = \{\mathsf{M}_i, i = 1,\ldots,\mu\}$, of μ alternative, competing, parameterized FE and prediction error model classes, and let $\underline{\theta}_i \in R^{N_{\theta_i}}$ be the free parameters of the model class M_i. The posterior probabilities $P(\mathsf{M}_i|D)$ of the various model classes given the data D is [14]

$$P(\mathsf{M}_i|D) = \frac{p(D|\mathsf{M}_i)P(\mathsf{M}_i)}{p(D|\mathsf{M}_{Fam})} \tag{8}$$

where $P(\mathsf{M}_i)$ is the prior probability and $p(D|\mathsf{M}_i)$ is the evidence of the model class M_i. The optimal model class M_{best} is selected as the one that maximizes $P(\mathsf{M}_i|D)$ given by (8). For the case where no prior information is available, the prior probabilities are assumed to be equal, $P(\mathsf{M}_i) = 1/\mu$, so the selection among the model classes is based solely on their evidence values.

The asymptotic approximations may fail to give a good representation of the posterior PDF in the case of multimodal distributions or for un-identifiable cases manifested for relatively large number of model parameters in relation to the information contained in the data. For more accurate estimates, one should use SSA to generate samples that populate the posterior PDF in (6). Among the SSA available, the TMCMC algorithm [18] is one of the most promising algorithms for selecting the most probable model class among competitive ones, as well as finding and populating with samples the importance region of interest of the posterior PDF, even in the unidentifiable cases and multi-modal posterior probability distributions. In addition, the TMCMC samples can be used to yield an estimate of the evidence $p(D|\mathsf{M}_i)$ in (8) required for model class selection [18,42]. The samples generated at the final stage of the algorithm can further be used for estimating the probability integrals encountered in robust prediction of various performance quantities of interest.

2.3. Computational aspects for linear FE models with large number of DOF

The computational demands in the aforementioned FE model updating methodologies depend highly on the number of FE analyses and the time required for performing a FE analysis. The optimal model in the proposed single-objective optimization, the Pareto models in the multi-objective optimization and the most probable model in the Bayesian asymptotic formulation can be estimated using available optimization algorithms. In particular, the optimization of $J(\underline{\theta};w)$ in (4) or $g(\underline{\theta},\sigma;w)$ in (7) can readily be carried out numerically using any available gradient-based algorithm for optimizing a nonlinear function of several variables. In addition, the set of Pareto optimal solutions can be obtained using the Normal-Boundary Intersection (NBI) method [11] which is a very efficient algorithm for solving the multi-objective optimization problem defined in (5). Each Pareto optimal solution is obtained by solving a single-objective optimization problem using gradient-based constrained optimization algorithms [10]. The computational time is of the order of the number of points used to represent the Pareto front multiplied by the computational time required to solve a single-objective optimization problem for computing each point on the front.

The gradient-based optimization algorithms require the estimation of the gradients of the residuals $J_1(\underline{\theta})$ and $J_2(\underline{\theta})$ defined in (1) and (2). This also contributes significantly to the time required to complete an iteration. Herein, Nelson method [43] is used to compute the gradients of the modal frequencies and mode shapes. The advantage of the Nelson's method compared to other methods (e.g. [44]) is that the gradients of the modal frequency and mode shape of a mode are computed from the modal frequency and mode shape of the same mode and there is no need to compute the modal frequencies and mode shapes from other modes. Using adjoint formulations [45], the computational demands for estimating the gradients of $J_1(\underline{\theta})$ and J_2 $(\underline{\theta})$ are independent of the number of parameters involved in the vector $\underline{\theta}$. The most time consuming operation arises from the solution of a linear system with the matrix of coefficients to be a slightly modified version of the symmetric, non-positive definite, matrix $K-\lambda_r M$. This requires the factorization for the modified $K-\lambda_r M$ matrices of the lowest $r = 1,\ldots,m$ modes involved in the residuals, contributing significantly to the overall computational effort at each iteration.

For objective functions in (4) or (7) involving multiple local/global optima, gradient based optimization algorithms may fail to converge to the global optimum. Stochastic optimization algorithms (e.g. [46–48]) are convenient tools for estimating the global optimum, avoiding premature convergence to a local one. These non-gradient based stochastic optimization algorithms require a significantly larger number of FE model re-analyses to be performed compared to the FE model analyses involved in gradient-based optimization algorithms, substantially increasing the computational demands.

Furthermore, Bayesian FE model updating techniques, based on SSA such as the efficient TMCMC algorithm, involve drawing a large number of samples for tracing and then populating the important region in the uncertain parameter space. Compared to the previous algorithms, TMCMC require a substantially larger number of FE model analyses since one FE analysis is required for each sample generated in the TMCMC algorithm. Consequently, the computational demands can become excessive when the computational time for performing a FE analysis is not negligible.

For FE models involving hundreds of thousands or even million DOF the computational demands for repeatedly solving the large-scale eigen-problems may be excessive. The objective of this work is to examine the conditions under which substantial reductions in the computational effort can be achieved by integrating dynamic reduction techniques into the FE formulations, aiming at reducing the sizes of the stiffness and mass matrices and eliminating the expensive re-analyses of components eigenproblems due to the variations of the system parameters, without compromising the solution accuracy.

We limit the formulation to the case for which the stiffness and mass matrices depend linearly on the model parameters $\underline{\theta}$. Specifically, it is assumed that the mass and stiffness matrix takes the form

$$K(\underline{\theta}) = K_0 + \sum_{i=1}^{N_\theta} K_j \theta_j$$
$$M(\underline{\theta}) = M_0 + \sum_{j=1}^{N_\theta} M_j \theta_j \tag{9}$$

where M_0, K_0, M_j and K_j, $j = 1,\ldots,N_\theta$, are constant matrices independent of $\underline{\theta}$. Also, we assume that each parameter in the vector $\underline{\theta}$ is associated to the stiffness property of the substructure. This is a case that is often encountered in practical applications of model updating and damage detection techniques.

3. Component mode synthesis

3.1. Formulation using fixed-interface modes

In CMS techniques [30,31], a structure is divided into several components. For each component, the unconstrained DOF are partitioned into the boundary DOF, denoted by the subscript b and the internal DOF, denoted by the subscript i. The boundary DOF of a component include only those that are common with the boundary DOF of adjacent components, while the internal DOF of a component are not shared with any adjacent component. The stiffness and mass matrices $K^{(s)} \in \mathbb{R}^{n^{(s)}\times n^{(s)}}$ and $M^{(s)} \in \mathbb{R}^{n^{(s)}\times n^{(s)}}$ of a component s are partitioned to blocks related to the internal and boundary DOF as follows

$$M^{(s)} = \begin{bmatrix} M_{ii}^{(s)} & M_{ib}^{(s)} \\ M_{bi}^{(s)} & M_{bb}^{(s)} \end{bmatrix} \quad \text{and} \quad K^{(s)} = \begin{bmatrix} K_{ii}^{(s)} & K_{ib}^{(s)} \\ K_{bi}^{(s)} & K_{bb}^{(s)} \end{bmatrix} \tag{10}$$

where the indices i and b are sets containing the internal and boundary DOF of the component. According to the Craig–Bampton fixed-interface mode method, the Ritz coordinate transformation $\underline{u}^{(s)} = \left[\underline{u}_i^{(s)T}, \underline{u}_b^{(s)T}\right]^T = \Psi^{(s)}\underline{p}^{(s)}$, where

$$\Psi^{(s)} = \begin{bmatrix} \Phi_{ik}^{(s)} & \Psi_{ib}^{(s)} \\ 0_{bk}^{(s)} & I_{bb}^{(s)} \end{bmatrix} \tag{11}$$

is used to relate the physical displacement coordinates $\underline{u}^{(s)} \in \mathbb{R}^{n^{(s)}}$ of the component to the generalized coordinates $\underline{p}^{(s)} = \left[\underline{p}_k^{(s)T}, \underline{p}_b^{(s)T}\right]^T \in \mathbb{R}^{\hat{n}^{(s)}}$, $\hat{n}^{(s)} = n_k^{(s)} + n_b^{(s)}$, using the kept fixed-interface normal modes $\Phi_{ik}^{(s)} \in \mathbb{R}^{n_i^{(s)}\times n_k^{(s)}}$ satisfying the eigen-problem

$$K_{ii}^{(s)}\Phi_{ik}^{(s)} = M_{ii}^{(s)}\Phi_{ik}^{(s)}\Lambda_{kk}^{(s)} \tag{12}$$

and the interface constrained modes $\Psi_{ib}^{(s)} \in \mathbb{R}^{n_i^{(s)}\times n_b^{(s)}}$ given by $\Psi_{ib}^{(s)} = -\left[K_{ii}^{(s)}\right]^{-1}K_{ib}^{(s)}$. The matrix $\Lambda_{kk}^{(s)} = diag\left(\lambda_1^{(s)},\ldots,\lambda_{n_k^{(s)}}^{(s)}\right) \in \mathbb{R}^{n_k^{(s)}\times n_k^{(s)}}$ is diagonal containing the eigenvalues $\lambda_j^{(s)}$, $j = 1,\ldots,n_k^{(s)}$, of the kept fixed-interface normal modes. The fixed-interface modes $\Phi_{ik}^{(s)}$ are considered to be mass normalized, satisfying $\Phi_{ik}^{(s)T}M_{ii}^{(s)}\Phi_{ik}^{(s)} = I_{kk}^{(s)}$ and $\Phi_{ik}^{(s)T}K_{ii}^{(s)}\Phi_{ik}^{(s)} = \Lambda_{kk}^{(s)}$.

The component's mass and stiffness matrices $\hat{M}^{(s)} \in \mathbb{R}^{\hat{n}^{(s)}\times\hat{n}^{(s)}}$ and $\hat{K}^{(s)} \in \mathbb{R}^{\hat{n}^{(s)}\times\hat{n}^{(s)}}$ in the new reduced set of generalized coordinates $\underline{p}^{(s)}$ are transformed as follows

$$\hat{M}^{(s)} = \Psi^{(s)T}M^{(s)}\Psi^{(s)} \quad \text{and} \quad \hat{K}^{(s)} = \Psi^{(s)T}K^{(s)}\Psi^{(s)} \tag{13}$$

with the partitions for the component mass matrices $\hat{M}_{kk}^{(s)} \in \mathbb{R}^{n_k^{(s)}\times n_k^{(s)}}$, $\hat{M}_{kb}^{(s)} \in \mathbb{R}^{n_k^{(s)}\times n_b^{(s)}}$, $\hat{M}_{bb}^{(s)} \in \mathbb{R}^{n_b^{(s)}\times n_b^{(s)}}$ and stiffness matrices $\hat{K}_{kk}^{(s)} \in \mathbb{R}^{n_k^{(s)}\times n_k^{(s)}}$, $\hat{K}_{kb}^{(s)} \in \mathbb{R}^{n_k^{(s)}\times n_b^{(s)}}$ and $\hat{K}_{bb}^{(s)} \in \mathbb{R}^{n_b^{(s)}\times n_b^{(s)}}$ given respectively by

$$\begin{aligned} \hat{M}_{kk}^{(s)} &= I_{kk}^{(s)} \\ \hat{M}_{kb}^{(s)} &= \hat{M}_{bk}^{(s)T} = \Phi_{ik}^{(s)T}M_{ii}^{(s)}\Psi_{ib}^{(s)} + \Phi_{ik}^{(s)T}M_{ib}^{(s)} \\ \hat{M}_{bb}^{(s)} &= \left(\Psi_{ib}^{(s)T}M_{ii}^{(s)} + M_{bi}^{(s)}\right)\Psi_{ib}^{(s)} + \Psi_{ib}^{(s)T}M_{ib}^{(s)} + M_{bb}^{(s)} \end{aligned} \tag{14}$$

and

$$\begin{aligned} \hat{K}_{kk}^{(s)} &= \Lambda_{kk}^{(s)} \\ \hat{K}_{kb}^{(s)} &= \hat{K}_{bk}^{(s)T} = 0_{kb}^{(s)} \\ \hat{K}_{bb}^{(s)} &= K_{bb}^{(s)} - K_{bi}^{(s)}\left[K_{ii}^{(s)}\right]^{-1}K_{ib}^{(s)} = K_{bb}^{(s)} + \Psi_{ib}^{(s)T}K_{ib}^{(s)} \end{aligned} \tag{15}$$

For convenience, the relationships (14) and (15) between the reduced and the original stiffness and mass matrices of a component,

with $\Lambda_{kk}^{(s)}$ and $\Phi_{ik}^{(s)}$ given by (12), can be written in compact form as $[\hat{K}^{(s)}, \hat{M}^{(s)}] = \mathsf{G}[K^{(s)}, M^{(s)}]$ using the operator G.

In the substructure assembly process, the vector $\underline{p} = [\underline{p}^{(1)T}, \ldots, \underline{p}^{(N_c)T}]^T \in \mathbb{R}^{n_p}$, $n_p = \sum_{s=1}^{N_c} \hat{n}^{(s)}$, of the generalized coordinates for all N_c components is introduced. Letting $\underline{q} = \left[\underline{p}_k^{(1)T}, \ldots, \underline{p}_k^{(N_c)T}, \underline{u}_b^T\right]^T \in \mathbb{R}^{n_q}$ be the vector that contains the independent generalized coordinates consisting of the fixed-interface modal coordinates $\underline{p}_k^{(s)}$ for each component and the physical coordinates $\underline{u}_b^T = \left[\underline{u}_b^{(1)T}, \ldots, \underline{u}_b^{(N_b)T}\right]^T$ at the N_b interfaces, where $\underline{u}_b^{(\ell)}$ contains the displacements at the DOF of the interface ℓ, the following transformation is introduced

$$\underline{p} = S\underline{q} \tag{16}$$

where the component coupling matrix $S \in \mathbb{R}^{n_p \times n_q}$ is a matrix of zeros and ones that couples the independent generalized coordinates $\underline{q}$ of the reduced system with the generalized coordinates of each component.

The assembled Craig–Bampton stiffness matrix $\hat{K}^{CB} \in \mathbb{R}^{n_q \times n_q}$ and mass matrix $\hat{M}^{CB} \in \mathbb{R}^{n_q \times n_q}$ for the reduced vector $\underline{q}$ of generalized coordinates are given by

$$\hat{K}^{CB} = S^T \begin{bmatrix} \hat{K}^{(1)} & 0 & 0 \\ 0 & \ddots & 0 \\ 0 & 0 & \hat{K}^{(N_c)} \end{bmatrix} S = \sum_{s=1}^{N_c} \mathsf{F}_s[\hat{K}^{(s)}] \tag{17}$$

$$\hat{M}^{CB} = S^T \begin{bmatrix} \hat{M}^{(1)} & 0 & 0 \\ 0 & \ddots & 0 \\ 0 & 0 & \hat{M}^{(N_c)} \end{bmatrix} S = \sum_{s=1}^{N_c} \mathsf{F}_s[\hat{M}^{(s)}] \tag{18}$$

where the new mathematical operator $\mathsf{F}_s[\hat{K}^{(s)}]$ is conveniently introduced by the second part of equation (17) as

$$\mathsf{F}_s[\hat{K}^{(s)}] = S^T blockdiag\left[0_{\hat{n}^{(1)}\hat{n}^{(1)}}, \ldots, 0_{\hat{n}^{(s-1)}\hat{n}^{(s-1)}}, \hat{K}^{(s)}, 0_{\hat{n}^{(s+1)}\hat{n}^{(s+1)}}, \ldots, 0_{\hat{n}^{(N_c)}\hat{n}^{(N_c)}}\right] S \tag{19}$$

where $0_{ij} \in \mathbb{R}^{i \times j}$ denotes a matrix of zeroes, and $blockdiag[\hat{K}^{(1)}, \ldots, \hat{K}^{(N_c)}] \in \mathbb{R}^{n_p \times n_p}$ denotes a block diagonal matrix having as diagonal blocks the matrices $\hat{K}^{(s)}$, $s = 1, \ldots, N_c$. The operator F_s will be used later to simplify the integration of the CMS into the FE formulation.

Solving the reduced eigen-problem

$$\hat{K}^{CB} Q = \hat{M}^{CB} Q \Lambda \tag{20}$$

associated with the reduced mass and stiffness matrices $\hat{M}^{CB}$ and $\hat{K}^{CB}$, respectively, one obtains the modal frequencies in $\Lambda = diag(\omega_i^2) \in \mathbb{R}^{n_q \times n_q}$ and the corresponding mode shape matrix $Q = [\hat{q}_1, \ldots, \hat{q}_{n_q}] \in \mathbb{R}^{n_q \times n_q}$ of the reduced system.

Introducing the constant matrix $\hat{S} \in \mathbb{R}^{N_0 \times n_p}$ to map the vector $[\underline{u}^{(1)T}, \ldots, \underline{u}^{(N_c)T}]$ of the physical coordinates for all structural components to the physical coordinates $\underline{u}$ of the structure at the N_0 measured DOF such that $\underline{u} = \hat{S}p$ and using (16), the physical mode shapes $\underline{\phi}_r \in \mathbb{R}^{N_0}$ of the original structure at the N_0 measured DOF are recovered from the mode shapes $\hat{q}_r \in \mathbb{R}^{n_q}$ of the reduced system as follows

$$\underline{\phi}_r = \hat{S}\Psi S\underline{\hat{q}}_r = \hat{L}\underline{\hat{q}}_r \tag{21}$$

where $\hat{L} = \hat{S}\Psi S \in \mathrm{R}^{N_0 \times n_q}$ and $\Psi = blockdiag[\Psi^{(1)}, \ldots, \Psi^{(N_c)}] \in \mathrm{R}^{n_p \times n_p}$.

3.2. Reduction of the interface DOF using characteristic interface modes

Further reduction in the generalized coordinates can be achieved by replacing the interface DOF by a reduced number of characteristic interface modes [49]. For this, the physical displacement coordinates $\underline{u}_b^{(\ell)} \in \mathbb{R}^{m_b^{(\ell)}}$ at an interface ℓ between two components are represented in terms of the generalized coordinates $\underline{\zeta}^{(\ell)} \in \mathbb{R}^{m_k^{(\ell)}}$ of the interface by the Ritz coordinate transformation

$$\underline{u}_b^{(\ell)} = V^{(\ell)} \underline{\zeta}^{(\ell)} \tag{22}$$

$\ell = 1, \ldots, N_b$, where the columns of $V^{(\ell)} \in \mathbb{R}^{m_b^{(\ell)} \times m_k^{(\ell)}}$ form the reduced basis of the $m_b^{(\ell)}$-dimensional space and $m_k^{(\ell)}$ is the number of elements in the basis.

The following transformation from the CMS generalized coordinates $\underline{q}$ to the reduced-order model generalized coordinates $\underline{v} = \left[\underline{p}_k^{(1)T}, \ldots, \underline{p}_k^{(N_s)T}, \zeta^{(1)T}, \ldots, \zeta^{(N_b)T}\right]^T \in \mathbb{R}^{n_r}$, $n_r = \sum_{s=1}^{N_c} n_k^{(s)} + \sum_{\ell=1}^{N_b} m_k^{(\ell)}$, that contains the kept fixed interface modes and the kept characteristic interface modes, is introduced as

$$\underline{q} = V\underline{v} \tag{23}$$

where $V = blockdiag(I_{n_k^{(1)}}, \ldots, I_{n_k^{(N_c)}}, V^{(1)}, \ldots, V^{(N_b)}) \in \mathbb{R}^{n_q \times n_r}$ and I_n denotes the identity matrix of dimension n. Using (23), the final reduced mass and stiffness matrices take the form $\hat{K} = V^T \hat{K}^{CB} V$ and $\hat{M} = V^T \hat{M}^{CB} V$ and the resulting eigenvalue problem at the reduced system level becomes

$$\hat{K}\Gamma = \hat{M}\Gamma\Lambda \tag{24}$$

where the diagonal matrix Λ contains the modal frequencies and the matrix $\Gamma \in \mathbb{R}^{n_r \times n_r}$ contains the corresponding n_r mode shapes of the reduced system.

The kept characteristic interface modes of the matrix $V^{(\ell)}$ satisfy the eigen-problem

$$\hat{K}^{CB}_{\hat{b}_\ell \hat{b}_\ell} V^{(\ell)} = \hat{M}^{CB}_{\hat{b}_\ell \hat{b}_\ell} V^{(\ell)} \Omega^{(\ell)} \tag{25}$$

where $\hat{b}_\ell$ is the index set denoting the positions of the generalized coordinates $\underline{u}_b^{(\ell)} \in \mathbb{R}^{m_b^{(\ell)}}$ in the vector $\underline{q}$ corresponding to the interface ℓ, while the stiffness and mass matrices $\hat{K}^{CB}_{\hat{b}_\ell \hat{b}_\ell} \in \mathbb{R}^{m_b^{(\ell)} \times m_b^{(\ell)}}$ and $\hat{M}^{CB}_{\hat{b}_\ell \hat{b}_\ell} \in \mathbb{R}^{m_b^{(\ell)} \times m_b^{(\ell)}}$ in (25) are the partitions of the reduced stiffness and mass matrices $\hat{K}^{CB}$ and $\hat{M}^{CB}$ associated with the coordinates $\underline{u}_b^{(\ell)}$ at the ℓ-th interface. These partitions are readily obtained from the corresponding partitions of the stiffness and mass matrices of the components connecting to the interface ℓ in the form

$$\hat{K}^{CB}_{\hat{b}_\ell \hat{b}_\ell} = \sum_{s \in C_\ell} \hat{K}^{(s)}_{b_\ell b_\ell} \quad \text{and} \quad \hat{M}^{CB}_{\hat{b}_\ell \hat{b}_\ell} = \sum_{s \in C_\ell} \hat{M}^{(s)}_{b_\ell b_\ell} \tag{26}$$

where C_ℓ is the integer set that contains the components that connect to the interface ℓ, and b_ℓ is the index set denoting the positions of the $\underline{u}_b^{(\ell)} \in \mathbb{R}^{m_b^{(\ell)}}$ corresponding to the interface ℓ in the vector $\underline{u}^{(s)}$ of the component s. Note that the stiffness matrix $\hat{K}$ of the reduced system is diagonal, given by $\hat{K} = diag\left(\Lambda_{kk}^{(1)}, \ldots, \Lambda_{kk}^{(N_c)}, \Omega_{kk}^{(1)}, \ldots, \Omega_{kk}^{(N_b)}\right)$, with diagonal elements the eigenvalues of each fixed interface and characteristic interface mode.

The components of the mode shape matrix $Q = [\underline{\hat{q}}_1, \ldots, \underline{\hat{q}}_{n_q}] \in \mathbb{R}^{n_q \times n_q}$ of the eigenvalue problem (20) are related to the components of the mode shape matrix $\Gamma = [\underline{\gamma}_1, \ldots, \underline{\gamma}_{n_r}] \in \mathbb{R}^{n_r \times n_r}$ of the eigenvalue problem (24) through the relationship $\underline{\hat{q}}_r = V\underline{\gamma}_r$. Specifically, using (21), the mode shapes

$\underline{\phi}_r$ of the original structure at the N_0 measured DOF are recovered from the mode shapes $\underline{\gamma}_r$ of the reduced system as follows

$$\underline{\phi}_r = \hat{S}\Psi S V \underline{\gamma}_r = \hat{L} V \underline{\gamma}_r = \tilde{L}\underline{\gamma}_r \tag{27}$$

where $\tilde{L} = \hat{L}V = \hat{S}\Psi S V \in \mathbb{R}^{N_0 \times n_r}$.

4. Model updating using CMS

The CMS procedure is next integrated into the FE model updating formulation. The linear dependence of the mass and stiffness matrices on the parameter vector $\underline{\theta}$ given in (9) implies that at the component level the mass and stiffness matrices as well as their partitions admit a similar representation, that is

$$\begin{aligned} K^{(s)} &= K_0^{(s)} + \sum_{j=1}^{N_\theta} K_j^{(s)} \theta_j \\ M^{(s)} &= M_0^{(s)} + \sum_{j=1}^{N_\theta} M_j^{(s)} \theta_j \end{aligned} \tag{28}$$

Attention is focused on two special cases of the parameterization (28) for a component s. In the first case it is assumed that the mass and stiffness matrix of a component s do not depend on the model parameters in $\underline{\theta}$. In this case one has that $K^{(s)} = K_0^{(s)}$ and $M^{(s)} = M_0^{(s)}$. The component fixed-interface and constrained modes are independent of the parameter values. Only a single analysis is required to estimate the fixed-interface and constrained modes for the particular component s. These component modes are computed once for a reference model and are then used in the iterations or TMCMC sampling schemes involved in model updating. The computational savings arise from the fact that the eigenvalue problem to compute the eigenvalues and mode shapes of the kept interface modes $\Phi_{ik}^{(s)}$ as well as the solution of the linear system to compute the constrained interface modes $\Psi_{ib}^{(s)}$ for a component s are not repeated at each iteration or TMCMC sampling point.

In the second case the stiffness matrix of a structural component s depends only on one model parameter, say θ_j, in the parameter vector $\underline{\theta}$, while the mass matrix $M^{(s)} = M_0^{(s)}$ is constant independent of $\underline{\theta}$. This case is enforced by dividing the structure into components based on the parameters introduced in the FE model for each physical substructure. Let Δ_j be the set of components that depend on the j-th variable θ_j. The stiffness matrix of a component $s \in \Delta_j$ takes the form

$$K^{(s)} = \overline{K}^{(s)} \theta_j \tag{29}$$

Equivalently, the relation (29) holds also for the partitions of the stiffness matrix. Substituting the partitions $K_{ii}^{(s)} = \overline{K}_{ii}^{(s)} \theta_j$ and $M_{ii}^{(s)} = M_{0,ii}^{(s)}$ in (12), it is readily derived that the matrix of the kept eigenvalues and eigenvectors of the component fixed-interface modes are given with respect to the parameter θ_j in the form

$$\Lambda^{(s)} = \overline{\Lambda}^{(s)} \theta_j \quad \text{and} \quad \Phi_{ik}^{(s)} = \overline{\Phi}_{ik}^{(s)} \tag{30}$$

where the matrices $\overline{\Lambda}^{(s)}$ and $\overline{\Phi}_{ik}^{(s)}$ are solutions of the following eigenproblem

$$\overline{K}_{ii}^{(s)} \overline{\Phi}_{ik}^{(s)} = M_{0,ii}^{(s)} \overline{\Phi}_{ik}^{(s)} \overline{\Lambda}_{kk}^{(s)} \tag{31}$$

and thus they are independent of the values of θ_j or the FE model variations at the component level due to changes in the model parameter. Also using the stiffness matrix partitions $K_{ii}^{(s)} = \overline{K}_{ii}^{(s)} \theta_j$ and $K_{ib}^{(s)} = \overline{K}_{ib}^{(s)} \theta_j$, the constrained modes are given by the constant matrix

$$\Psi_{ib}^{(s)} = -\left[K_{ii}^{(s)}\right]^{-1} K_{ib}^{(s)} = -\left[\overline{K}_{ii}^{(s)}\right]^{-1} \overline{K}_{ib}^{(s)} \tag{32}$$

also independent of the values of the parameter θ_j or FE model variations at component level. Thus, a single component analysis is required to provide the exact estimate of the fixed-interface modes from (30) and the constrained modes from (32) for any value of the model parameter θ_j.

Substituting into the reduced mass and stiffness matrices (14) and (15) the partitions of the stiffness matrix (29), the eigenproperties (30) and the interface constraint modes (32) of the component s, it is straightforward to verify that the reduced stiffness matrix of component s takes the form

$$\hat{K}^{(s)} = \hat{\overline{K}}^{(s)} \theta_j \tag{33}$$

where the reduced matrix $\hat{\overline{K}}^{(s)}$ and the reduced mass matrix $\hat{M}^{(s)}$ are constant matrices given by $[\hat{\overline{K}}^{(s)}, \hat{M}^{(s)}] = \mathsf{G}[\overline{K}^{(s)}, M_0^{(s)}]$, independent of the values of the model parameters $\underline{\theta}$.

Introduce next the index set Σ to contain the structural components s that depend on a parameter in the vector $\underline{\theta}$. Then the set $\overline{\Sigma} = \{1, \ldots, N_c\} - \Sigma$ contains the component numbers for which their properties are constant and independent on the values of the parameter vector $\underline{\theta}$. Substituting (33) into (17), the stiffness matrix of the Craig–Bampton reduced system admits the representation

$$\hat{K}^{CB} = \hat{K}_0^{CB} + \sum_{j=1}^{N_\theta} \hat{K}_j^{CB} \theta_j \tag{34}$$

and the mass matrix is given by $\hat{M}^{CB} = \hat{M}_0^{CB}$, where the coefficient matrices $\hat{K}_0^{CB}$ and $\hat{K}_j^{CB}$ in the expansion (34) are assembled from the component stiffness matrices, defined in (33), by

$$\hat{K}_0^{CB} = \sum_{s \in \overline{\Sigma}} \mathsf{F}_s[\hat{K}^{(s)}] \text{ and } \hat{K}_j^{CB} = \sum_{s \in \Delta_j} \mathsf{F}_s[\hat{\overline{K}}^{(s)}] \tag{35}$$

The sum in the second of (35) takes into account that more than one components $s \in \Delta_j$ may depend on the parameter θ_j.

It is important to note that the assembled matrices $\hat{K}_0^{CB}$ and $\hat{K}_j^{CB}$ of the Craig–Bampton reduced system in the expansion (34) are independent of the values of $\underline{\theta}$. In order to save computational time, these constant matrices are computed and assembled once and, therefore, there is no need this computation to be repeated during the iterations involved in optimization or TMCMC sampling algorithms for model updating due to the changes in the values of the parameter vector $\underline{\theta}$. This aforementioned procedure results in substantial computational savings since it avoids (a) re-computing the fixed-interface and constrained modes for each component, and (b) assembling the reduced matrices from these components. The formulation guarantees that the reduced system is based on the exact component modes for all values of the model parameters. In addition, using (21) and the fact that $\Psi^{(s)}$ and thus Ψ are independent of $\underline{\theta}$, the observation matrix $\hat{L} = \hat{S}\Psi S$ in (21) is constant, independent of the parameter vector $\underline{\theta}$.

The modal frequency and mode shape residuals involved in the objective $J(\underline{\theta}; w)$ have the same exactly form as in (1) and (2) with $\underline{\varphi}_r(\underline{\theta})$ and the constant matrix L in $\underline{\phi}_r(\underline{\theta}) = L\underline{\varphi}_r(\underline{\theta})$ be replaced by $\underline{\hat{q}}_r(\underline{\theta})$ and the constant matrix $\hat{L} = \hat{S}\Psi S$, respectively. Available model updating formulations and software can thus be readily used to handle the parameter estimation by just replacing the eigenvalue problem (3) of the original mass and stiffness matrices with the eigenvalue problem (20) of the reduced system matrices with $\hat{K}^{CB}(\underline{\theta})$ given by (34) and $\hat{M}^{CB}(\underline{\theta}) = \hat{M}_0^{CB}$, as well as replacing the constant matrix L of zeros and ones by the constant matrix $\hat{L} = \hat{S}\Psi S$.

Special attention should be given when the size of the reduced mass and stiffness matrices are dominated by a large number of interface DOF. In this case, the coordinate transformation (22) can be used to further reduce the number of interface DOF for one or more interfaces. Using (26), it is clear that the stiffness

matrix of the eigenvalue problem involved in (25) depends on the parameters associated with the components that connect to the interface ℓ. The variability of these parameters affects the characteristic interface modes $V^{(\ell)}$ which are functions of these parameters. Exact estimates of the characteristic interface modes in iterative or TMCMC sampling algorithms can only be obtained by repeatedly solving (25) for each different value of the respective parameters. For large number of DOF at the interface, such re-analyses at the interface level may increase substantially the computational demands. Interpolation schemes [37] can be used to approximate the characteristic interface modes at the interface level in terms of the characteristic interface modes at a number of support points in a significantly reduced space of model parameters associated with the components that connect to the interface ℓ.

Alternatively, selecting $V^{(\ell)}$ in (22) to be constant, independent of $\underline{\theta}$, the formulation significantly simplifies, with the reduced stiffness matrix to be given by

$$\hat{K} = \hat{K}_0 + \sum_{j=1}^{N_\theta} \hat{K}_j \theta_j \tag{36}$$

where $\hat{K}_0 = V^T \hat{K}_0^{CB} V$ and $\hat{K}_j = V^T \hat{K}_j^{CB} V$ are constant matrices, while the reduced mass matrix be given by the constant matrix $\hat{M}_0 = V^T \hat{M}_0^{CB} V$. The modal frequency and mode shape residuals involved in the objective function $J(\underline{\theta}; w)$ in the model updating formulations have exactly the same form as in (1) and (2) with $\underline{\varphi}_r(\underline{\theta})$ and the constant matrix L in $\underline{\phi}_r(\underline{\theta}) = L\underline{\varphi}_r(\underline{\theta})$ be replaced by $\underline{\gamma}_r(\underline{\theta})$ defined in (24) and the constant matrix $\tilde{L} = \hat{S}\Psi S V$ defined in (27), respectively. The choice of constant $V^{(\ell)}$ is critical in order to get accurate results with the least number of characteristic interface modes over the region of variation of the model parameters associated with the interface ℓ. In FE model updating, the $V^{(\ell)}$ can be chosen as the eigenvectors of the lowest modes of the eigenvalue problem (25) corresponding to a reference model of the structure, avoiding the computational cost involved with the repetitive solution of (25) at each iteration or TMCMC sample. This, however, may deteriorate the accuracy of the predictions for large variations of the model parameters. To improve convergence and maintain the accuracy of the final optimal estimate in iterative optimization algorithms, the reduced basis forming $V^{(\ell)}$ can be updated every few iterations. Also, to maintain higher level of accuracy in the TMCMC sampling algorithm, the reduced basis forming $V^{(\ell)}$ can be kept constant within a TMCMC stage, with this basis selected to correspond to the most probable model predicted from the previous TMCMC stage. Such technique is expected to give sufficiently accurate results for the final TMCMC stage, especially for the cases where the posterior PDF is isolated in a relative small region in the parameter space. The computational efficiency and accuracy of reducing the interface DOF using constant $V^{(\ell)}$ will be demonstrated in the application section.

It should be pointed out that the significant savings arising partly from the reduction of the size of the eigenvalue problem from n to n_r in the proposed model reduction technique and partly from the fact that the estimation of the the component fixed-interface modes and the characteristic interface modes need not to be repeated for each iteration involved in the optimization or TMCMC sampling algorithms. Moreover, for gradient-based optimization algorithms required in model updating schemes, further computational savings are obtained due to the reduction of the size of the matrix of the linear system that needs to be factorized in the adjoint formulation [45], from the size n for the full matrices $K - \lambda_r M$ to the size n_r for the reduced-order matrices $\hat{K} - \lambda_r \hat{M}$.

Attention should also be paid on the optimal number of components that should be used to represent a substructure with stiffness that depends linearly on a single parameter. More components within such substructure introduce extra interface DOFs or characteristic interface modes which increase the size and affect the sparsity structure of the reduced matrices $\hat{K}$ and $\hat{M}$. The total size of the reduced matrices is also affected by the number of the fixed interface modes for all components introduced for the substructure. From the computational point of view, the optimal choice of components for such a substructure would be to select the number of components and the optimal spatial division which will result in a reduced system that requires the least computational time for analysis. However, as the number of interface DOFs or characteristic interface modes increases by the introduction of more components per substructure, it is unlikely that the resulting increase in the size of the reduced matrices be effectively compensated by a decrease in the total number of fixed interface modes arising from the multiple components that represent the single substructure. Thus, in case where detailed optimal component selection studies are not available, the wisest choice is to select a single component per substructure.

As a final note, it is worth mentioning the treatment of a component in the CMS process for the general case for which the component stiffness and mass matrices depends on two or more parameters in the vector $\underline{\theta}$. In these cases, in order to obtain exact estimates of the component modes, the solution of the eigenvalue problems for such a component is not avoided. The fixed-interface and characteristic interface modes have to be recomputed in each iteration or TMCMC sample involved in the model updating procedure and used to form the reduced stiffness and mass matrices of the components. This repeated computation, however, is usually confined to a small number of components. Interpolation schemes can also be adopted to avoid re-analyses at the component or interface level by approximating the fixed interface modes and/or the characteristic interface modes at various values of the model parameters in terms of the corresponding modes of a family of models defined at a number of support points in the parameter space [37]. However, it should be pointed out that the use of interpolating schemes for approximating the fixed interface and the characteristic interface modes is an open issue and further analyses are required to evaluate the effectiveness of such techniques in the general case.

5. Applications

The purpose of the application is to demonstrate the applicability, computational efficiency and accuracy of the proposed model reduction technique for FE model updating. For this, a model of

Fig. 1. General view of Metsovo bridge.

the Metsovo bridge shown in Fig. 1 is updated. The bridge is the highest reinforced concrete bridge of Egnatia Odos motorway located in Greece, with the height of the taller pier P2 equal to 110 m. The total length of the bridge is 537 m. The bridge has 4 spans, of length 44.78 m, 117.87 m, 235.00 m, 140.00 m and three piers of which pier P1, 45 m high, supports the boxbeam superstructure through pot bearings (movable in both horizontal directions), while P2 and P3 piers (110 m and 35 m, respectively) connect monolithically to the superstructure. The total width of the deck is 13.95 m. The superstructure is prestressed of single boxbeam section, of height varying from the maximum 13.5 m in its support to pier P2 to the minimum 4.00 m in key section. Piers P2 and P3 are founded on huge circular Ø12.0 m rock sockets in the steep slopes of the Metsovitikos river, in a depth of 25 m and 15 m, respectively.

The commercial software package COMSOL Multiphysics [50] is used for developing the FE model of the bridge. For this, the structure was first designed in CAD environment and then imported in COMSOL Multiphysics modeling environment. The models were constructed based on the design plans, the geometric details and the material properties of the structure. The following nominal values of the material properties of the concrete deck, piers and foundations are considered. For the concrete deck, the nominal value of the Young's modulus is taken to be $E = 37$ Gpa, the Poison's ratio $\nu = 0.2$ and the density $\rho = 2548$ kg/m^3. For the piers and the foundation the nominal value of the Young's modulus is taken to be $E = 34$ GPa. A detailed FE model is created using three-dimensional tetrahedron quadratic Lagrange finite elements to model the whole bridge. An extra coarse mesh with quadratic Lagrange elements are chosen to predict the lowest 20 modal frequencies and mode shapes of the bridge. The selected model has 97,636 finite elements and 562,101 DOF.

5.1. Effectiveness of CMS technique

For demonstration purposes, the bridge is divided into nine physical components shown schematically in Fig. 2. Six components are related to the four spans of the bridge deck, while three components are related to the three piers. The eight interfaces between the components are also shown in Fig. 2. Each deck component consists of several 4–5 m deck sections. A typical 5 m section is shown in Fig. 3(a) along with its FE mesh. The tallest pier also consists of several sections. A typical 4 m pier section is also shown in Fig. 3(b) along with its FE mesh. It should be noted that the size of the elements in the FE mesh is the maximum possible one that can be considered, with typical element length of the order of the thickness of the deck cross-section. The entire simulation for assembling the mass and stiffness matrices of the structure or its components is performed within the COMSOL Multiphysics modeling environment and exported in Matlab environment for further processing using CMS techniques and FE model updating software.

The cut-off frequency ω_c is introduced to denote the highest modal frequency value that is of interest in FE model updating. In this study the cut-off frequency is selected to be equal to the 20th modal frequency of the nominal model. For the specific model, this frequency is obtained from modal analysis to be $\omega_c = 4.6$ Hz. The effectiveness of the CMS technique as a function of the number of modes retained for each component is next evaluated. For each component it is selected to retain all fixed interface modes that have frequency less than $\omega_{\max} = \rho\omega_c$, a multiple of the cut-off frequency ω_c, where the value of the multiplication factor ρ affects computational efficiency and accuracy of the model reduction technique. Representative values of ρ range from 2 to 10. The total number of internal DOF and retained modes for $\rho = 8$, $\rho = 5$ and $\rho = 2$ within all the components are reported in the second row of Table 1. The total number of internal and boundary DOF of the unreduced model are reported in the second column of Table 1 based on the components and interfaces shown in Fig. 2. The total number of internal DOF per component and the number of modes retained per component for different ρ values is shown in Fig. 4. It is clear from the results in Table 1 and Fig. 4 that a more than three orders of magnitude reduction in the number of DOF per component is achieved using CMS. For the case $\rho = 8$, a total of 286 internal modes out of the 558,801 are retained for all 9 components. Fig. 5 shows the fractional error between the modal frequencies computed using the complete FE model and the modal frequencies computed using the CMS technique as a function of the mode number for $\rho = 2$, 5 and 8. It can be seen that the fractional error for the lowest 20 modes fall below 10^{-4} for $\rho = 8$, 10^{-3} for $\rho = 5$ and 10^{-2} for $\rho = 2$, which ensures high levels of accuracy.

The total number of DOF of the reduced model $\rho = 8$ is 3586 which consist of 286 fixed interface generalized coordinates and 3300 constraint interface DOF for all components. It is thus obvious that a large number of generalized coordinates for the reduced

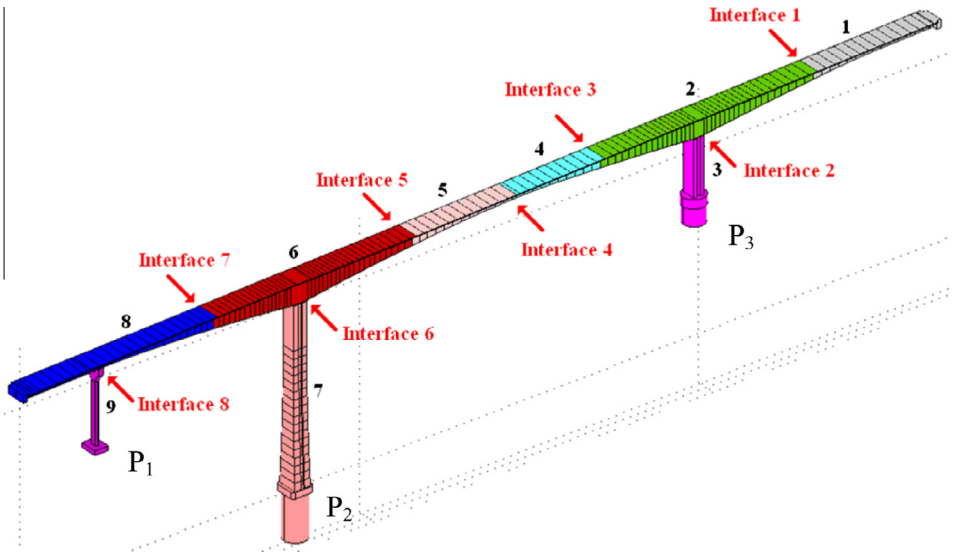

Fig. 2. Components of FE model of Metsovo bridge.

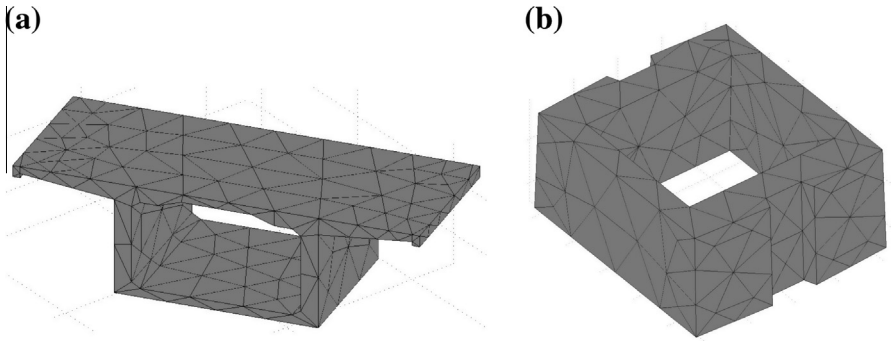

Fig. 3. (a) A typical 5 m section of the deck with its FE mesh, (b) a typical 4 m section of the tallest pier with its FE mesh.

Table 1
Total number of internal and interface DOF for the full (unreduced) and reduced models.

	Structure without reduction	Retained modes $\rho = 8$, $v = 200$	Retained modes $\rho = 5$, $v = 200$	Retained modes $\rho = 2$, $v = 200$
Total internal DOF	558,801	286	100	31
Total interface DOF	3300	306	306	306
Total DOF	562,101	592	406	337

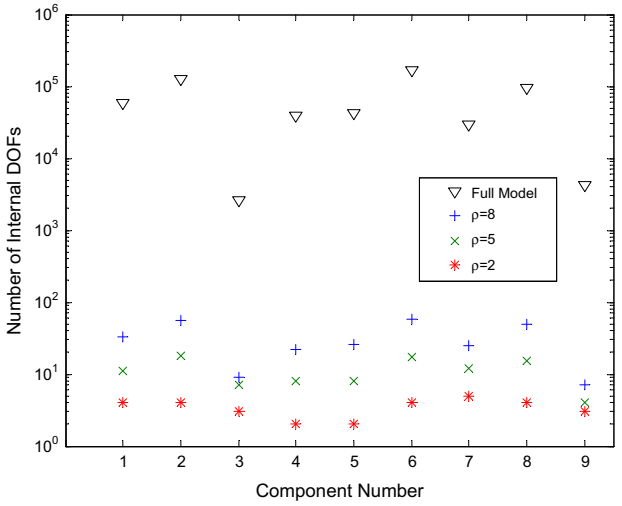

Fig. 4. Number of DOF per component of the FE model of Metsovo bridge.

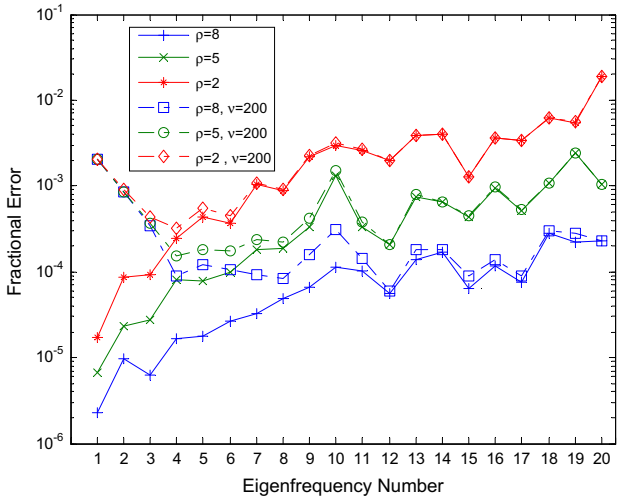

Fig. 5. Fractional modal frequency error between the predictions of the full model and the reduced model as a function of eigenmode number and for different values of ρ and v.

system arises from the interface DOF. A further reduction in the number of generalized coordinates for the reduced system can be achieved by retaining only a fraction of the constrained interface modes. The number of DOF per interface is shown in the third column of Table 2. For each interface defined in Table 2, it is selected to retain all modes that have frequency less than $\omega_{\max} = v\omega_c$, a multiple of the cutoff frequency ω_c, where the multiplication factor v is user and problem dependent. The number of modes retained per interface for $v = 200$ is given in the last column of Table 2. The number of retained interface modes is approximately 10% of the interface DOF for each interface. Fig. 5 presents results for the fractional error between the modal frequencies computed using the CMS method with retained characteristic interface modes for $v = 200$ for each interface and the modal frequencies computed using the complete FE model as a function of the mode number. It can be seen that the fractional error for most of the lowest 20 modes of the structure fall well below 10^{-3} for $v = 200$ and ρ values as low as $\rho = 5$. Thus, the value of $v = 200$ gives accurate results in this case, while the number of retained interface

Table 2
Information for each interface involved in the modeling with number of interface DOF and retained modes for $v = 200$.

Interfaces	Adjacent components	Interface DOF	Retained modes $v = 200$
1	1–2	441	46
2	2–3	258	27
3	2–4	432	47
4	4–5	441	42
5	5–6	423	46
6	6–7	660	33
7	6–8	495	49
8	8–9	150	16
Total DOF or retained modes		3300	306

modes for all interfaces is 306 which corresponds to 10% of the total number of interface DOF. The reduced system for $\rho = 5$ and

$v = 200$ has 406 DOF from which 100 generalized coordinates are fixed-interface modes for all components and the rest 306 generalized coordinates are characteristic interface modes for all 8 interfaces. Obviously the number of generalized coordinates is drastically reduced by more than three orders of magnitude compared to the number of DOF of the original unreduced FE model. The significant reduction in number of generalized coordinates of the reduced system and the increased accuracy of the results are promising for using the proposed model reduction method in FE model updating.

5.2. FE model updating using single- and multi-objective optimization

For demonstration purposes, the FE model is parameterized using five parameters associated with the modulus of elasticity of one or more structural components shown in Fig. 2. The parameterization is graphically depicted in Fig. 6(a). Specifically, the first two parameters θ_1 and θ_2 account respectively for the modulus of elasticity of the pier components 3 and 7 of the bridge. The parameter θ_3 accounts for the modulus of elasticity of the components 1 and 2 of the deck, the parameter θ_4 accounts for the components 4 and 5, while the parameter θ_5 accounts for the components 6 and 8. Note that for the three substructures parameterized by a single parameter θ_3, θ_4 or θ_5, two components per substructure have been introduced, demonstrating the flexibility of the proposed methodology. The component 9 is not parameterized. The parameters are introduced to scale the nominal values of the properties that they model so that the value of the parameters equal to one correspond to the nominal value of the FE model. The nominal FE model corresponds to values of $\theta_1 = \cdots = \theta_5 = 1$.

For the purpose of the present analysis, simulated, noise contaminated, measured modal frequencies $\hat{\omega}_r^2$ and mode shapes $\hat{\varphi}_r$ are generated by perturbing the values of the modal properties $\omega_{0,r}$ and $\varphi_{0,r}$, corresponding to the nominal FE model for $\underline{\theta} = 1$, according to the expressions $\hat{\omega}_r^2 = \omega_{0,r}^2(1 + n_r)$ and $\hat{\varphi}_r = \varphi_{0,r} + \|\varphi_{0,r}\|\underline{e}_r$, where $n_r \sim N(0,s^2)$ are samples from a zero-mean normal distribution with variance s^2, and $\underline{e}_r$ is a zero-mean normal random vector with diagonal covariance matrix $e^2 I$. The standard deviations s and e of the perturbed terms control mainly the size of the model and measurement errors for the modal frequencies and the mode shapes. The assumed constant noise level for the different modeshape components may not exactly reflect the actual differences observed in real applications between the predictions from a model and the actual behavior of the structure since model error will cause dissimilar noise levels at different modeshape components. However, for the purpose of this study, which is to demonstrate the efficiency of the proposed CMS scheme, the addition of constant noise level to different modeshape components is sufficient. Herein, the magnitudes of the error terms are chosen to be $s = 1\%$ and $e = 3\%$.

The FE model is updated using the simulated modal data for the lowest 10 modes. A sensor configuration involving 36 sensors is considered. The sensors are placed along the deck and the piers at the locations and directions as shown in Fig. 6(b), measuring along the longitudinal, transverse and vertical directions.

To investigate the accuracy and computational efficiency of the proposed CMS formulation, the FE model updating is first performed using the single objective optimization method by selecting the weight in (4) to be $w = 1$. Results for the accuracy of the model parameters and the computational effort are presented in Table 3 for the following six cases involving different reduction schemes in internal and boundary DOF: (a) $\rho = 8$, (b) $\rho = 5$, (c) $\rho = 2$, (d) $\rho = 8$ and $v = 200$, (e) $\rho = 5$ and $v = 200$, and (f) $\rho = 2$ and $v = 200$. The initial values of the parameters used to carry out the optimization are $\theta_i = 1.2$, $i = 1,\ldots,5$. The errors in the fourth column of the table are defined by the norm $\sqrt{\|(\underline{\theta}^{est} - \underline{\theta}^{full})/\underline{\theta}^{full}\|_2/N_\theta} \times 100$ of the fractional errors of the optimal model parameter estimates $\underline{\theta}^{est}$ obtained from the CMS-reduced FE model and the optimal estimates $\underline{\theta}^{full}$ obtained from the full (non-reduced) FE model. The percentage difference of the

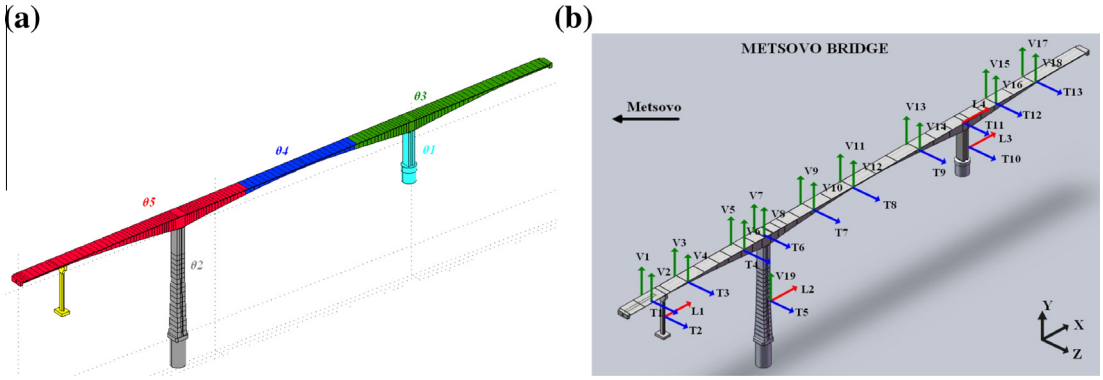

Fig. 6. (a) FE model parameterization based on 5 parameters, (b) sensor configuration involving 36 sensors.

Table 3
Accuracy and computational effort for FE model updating based on full and reduced order models of Metsovo bridge.

Cases	FE models	Total DOF	Single-objective optimization			Multi-objective optimization
			Error (%)	Function evaluations	Time (sec)	Time (sec)
Full	Full model	562,101	0.00	8	14,251	321,352
(a)	$\rho = 8$	3586	0.03	14	766	15,050
(b)	$\rho = 5$	3400	0.43	13	677	12,282
(c)	$\rho = 2$	3331	0.17	13	674	11,437
(d)	$\rho = 8$, $v = 200$	592	0.11	14	12	197
(e)	$\rho = 5$, $v = 200$	406	0.46	13	8	128
(f)	$\rho = 2$, $v = 200$	337	0.24	13	6	109

optimal estimates for the full model from the values $\underline{\theta} = 1$ of the nominal model is $(\underline{\theta}^{full} - \underline{1})^T \times 100 = (0.57, 1.87, 1.09, 0.61, 1.21)^T$ and it is due to the noisy data considered. The results in Table 3 clearly suggest that the error in the estimates of the model parameters is very small for the case of reducing the internal DOF using $\rho = 8$, $\rho = 5$ and $\rho = 2$. The fluctuation in the values of the parameters errors reported in Table 3 as a function of the ρ values should not be surprising since, due to the noise added, the experimental modal data do not coincide with the modal data predicted by the unreduced model.

The number of function evaluations and the computational effort are also shown in Table 3. The computational time for carrying out the optimization for the reduced-order models is 5% of the time required for the full model. Consequently, significant gains in computational effort are achieved without sacrificing the accuracy in the model parameter estimates. A further reduction in the computational effort, close to two order of magnitude, is achieved by reducing the interface degrees of freedom using $v = 200$, while the accuracy is maintained to acceptable levels since the errors are smaller than 0.46%. Overall, for $\rho = 8$ and $v = 200$, the computational effort is drastically reduced by three to four orders of magnitude, without sacrificing in accuracy since the error norm is 0.11%.

Results are next presented for the multi-objective model updating framework. Figs. 7 and 8 present the Pareto front and the Pareto optimal models, respectively, computed using the full FE model and the six reduced-order models introduced before. The Pareto front and optimal solutions are represented by 20 points computed by the Normal Boundary Intersection algorithm [11]. It is clear from Fig. 8, that the quality of the estimates provided is excellent for the reduced-order models (a) and (d), very good for the reduced-order models (b) and (e), and acceptable for the reduced-order models (c) and (f). The computational effort for performing the FE model updating using the full and reduced-order models is reported in the last column of Table 3. The computational time required to carry out the multi-objective optimization for obtaining the Pareto optimal models using the full FE model is of the order of 89 h (approximately four days). Compared to the full model, the computational demands are substantially reduced by a factor of 20 for the reduced models (a) and (b), and by more than three orders of magnitude for the reduced models (d) and (e). Specifically, the computational time is 3–4 h when only the internal DOF of each component are reduced and 2–3 min when both internal and interface DOF are reduced. A drastic reduction in computational effort is thus achieved by using the reduced-order models, without sacrificing in accuracy of the model parameter estimates as shown in Figs. 7 and 8.

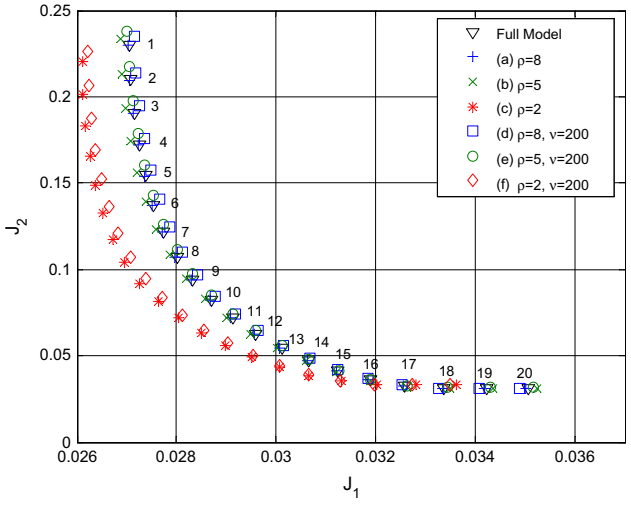

Fig. 7. Comparison of Pareto fronts for the full and reduced-order FE models.

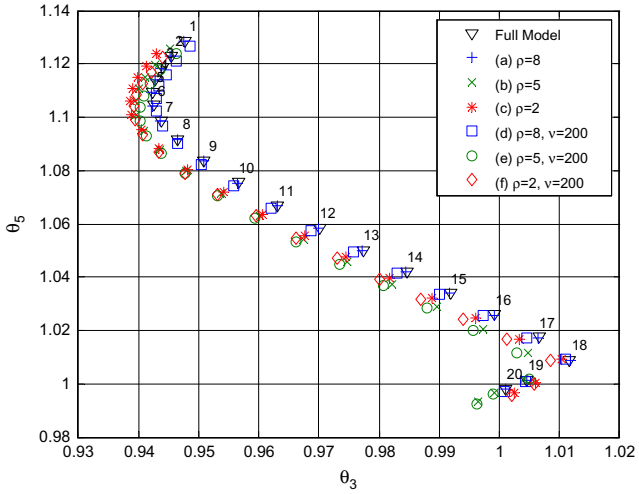

Fig. 8. Comparison of Pareto models in the 2-d projection (θ_3 ,θ_5) of the 5-d parameter space for the full and reduced-order FE models.

5.3. Application to damage identification using the Bayesian formulation

The proposed model reduction technique is well suited in damage identification applications that are based on FE model updating. This is illustrated next using the Bayesian method for structural damage identification proposed in Ntotsios et al. [22]. Specifically, a structure is divided into a number of substructures and it is assumed that damage in the structure is confined in one or more substructures, causing stiffness reduction in these damaged substructures. In order to identify which substructure contains the damage and predict the level of damage, a family of μ model classes $M_1, \ldots, M_\mu$ is introduced, and the damage identification is accomplished by associating each model class to damage contained within a substructure. For this, each model class M_i is parameterized by a number of structural model parameters $\underline{\theta}_i$ controlling the stiffness in the substructure i, while all other substructures are assumed to have fixed stiffness values equal to those corresponding to the undamaged structure. Damage in the substructure i will cause stiffness reduction which will alter the measured modal characteristics of the structure. The model class M_i that "contains" the damaged substructure i will be the most likely model class to observe the modal data since the parameter values $\underline{\theta}_i$ can adjust to the modified stiffness distribution of the substructure i, while the other modal classes that do not contain the substructure i are expected to provide a poor fit to the modal data.

Using the Bayesian model selection framework, the model classes are ranked according to the posterior probabilities based on the modal data identified from measurements. The most probable model class M_{best} that maximizes $P(M_i|D)$ in (8), through its association with a damage scenario on a specific substructure, will be indicative of the substructure that is damaged, while the posterior PDF of the model parameters of the corresponding most probable model class M_{best}, compared to the parameter values of the undamaged structure, will be indicative of the severity of damage in the identified damaged substructure.

To demonstrate the methodology, the Metsovo bridge is divided into 15 substructures as shown in Fig. 9. A number of competitive model classes $M^{[i]}$ and $M^{[i,j]}$ are introduced to monitor various

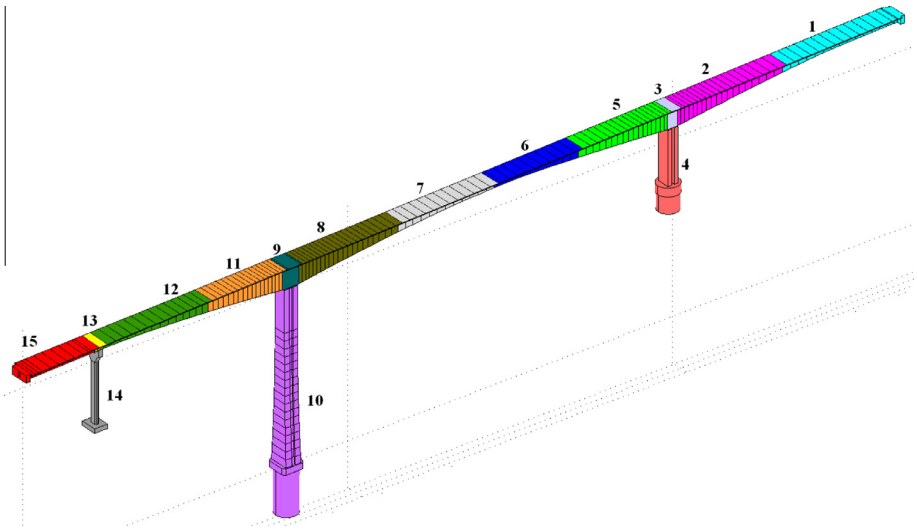

Fig. 9. Substructures of FE model of Metsovo bridge used for damage identification.

probable damage scenarios for the bridge corresponding to single and multiple damages at different substructures. The model class $M^{[i]}$ contains one parameter related to the stiffness (modulus of elasticity) of substructure i shown in Fig. 9. It can monitor damage associated with the stiffness reduction in the i substructure. The model class $M^{[i,j]}$ contains two parameters related to the stiffness of substructures i and j in Fig. 9. It can monitor damage associated with the stiffness reduction in either substructures i and j or simultaneously at both substructures. The five-parameter model shown in Fig. 6(a) is also included in the family of model classes to monitor simultaneous damages at five different substructures. This five-parameter model class is denoted by $M^{[5-par]}$. All model classes are generated from the updated FE model of the undamaged structure. For each model class, CMS techniques are used to alleviate the computational burden associated with the model updating problems that needs to be solved. For this, two different cases of reduced-order FE models are considered. The first case corresponds to models obtained by reducing the internal DOF using $\rho = 8$, while the second case corresponds to models obtained by reducing both the internal and interface DOF using $\rho = 8$ and $v = 200$. The Ritz basis for reducing the interface DOF were selected to be the characteristic interface modes obtained from Eq. (25) for the reference values $\underline{\theta} = 1$.

The number of components introduced for each model class depends on the parameterization. Specifically, the model class $M^{[i]}$ is divided into two, three or four components. One component is selected to be the substructure i shown in Fig. 9, while the remaining components are selected to be the parts of the remaining structure that connect to the interfaces of component i. The model classes $M^{[1]}$, $M^{[10]}$, $M^{[14]}$ and $M^{[15]}$ have one interface, the model classes $M^{[2]}$, $M^{[5]}$ to $M^{[8]}$, $M^{[11]}$ and $M^{[12]}$ have two interfaces, while the model classes $M^{[3]}$, $M^{[9]}$ and $M^{[13]}$ have three interfaces with the remaining structure. A similar division into components is introduced for the family of $M^{[i,j]}$ model classes. For example, model class $M^{[10,8]}$ is divided into four components, the first two components coincide with the physical substructures 10 and 8, the third includes the physical substructures 9, 11 to 15 and the fourth includes the substructures 1 to 7. The components in the $M^{[5-par]}$ model class are kept the same as the ones used in Section 5.2. The reduced stiffness matrices $\hat{K}_0$ and $\hat{K}_j$ in the linear representation (36) and the mass matrix $\hat{M}_0$ are assembled once for each model class and are stored in a database of model classes.

For investigating the computational efficiency and accuracy of the reduced models, a simulated damage is introduced at the highest pier (substructure 10 in Fig. 9), manifested as a stiffness reduction of 30% the nominal stiffness value. Simulated, noise

Table 4
Damage identification results, model DOF, number of FE simulations (NFES) and computational effort (CE) in minutes for each model class.

Model class	Evidence $\rho = 8$ (log)	Evidence $\rho = 8$ $v = 200$ (log)	$\Delta\theta_i$ $\rho = 8$ (%)	$\Delta\theta_i$ $\rho = 8$ $v = 200$ (%)	DOF (NFES) $\rho = 8$	DOF (NFES) $\rho = 8$ $v = 200$	CE $\rho = 8$ (min)	CE $\rho = 8$ $v = 200$ (min)
$M^{[2]}$	954.46	954.93	+27.9	+26.5	1724 (8000)	438 (8000)	123	3.5
$M^{[4]}$	954.99	955.08	−15.7	−15.2	989 (8000)	381 (8000)	42	3
$M^{[5]}$	988.17	989.32	−47.8	−47.3	1747 (9000)	441 (9000)	134	3.6
$M^{[8]}$	1005.5	1006.4	−31.3	−30.8	1824 (9000)	408 (9000)	170	0.5
$M^{[10]}$	1723.1	1723.3	−29.2	−29.2	1393 (12,000)	388 (12,000)	173	4.6
$M^{[10,7]}$	1722.5	1723.1	−29.0	−29.0	1829 (14,000)	425 (13,000)	245	5.4
			+4.0	+3.9				
$M^{[10,8]}$	1718.7	1719.0	−29.0	−29.0	2485 (14,000)	433 (13,000)	509	5.5
			+1.9	+1.3				
$M^{[5-par]}$	1700.4	1698.2	−1.3	−0.5	3,586 (19,000)	592 (19,000)	759	14
			−28.3	−28.5				
			+1.0	+0.9				
			+2.3	+1.5				
			+0.5	+0.5				
Total							2155	40.1

contaminated, measured modal frequencies and mode shapes are generated for the damaged structure by adding a 1% and 3% Gaussian noise to the modal frequencies and modeshape components generated from the nominal non-reduced FE model with 30% reduction of the stiffness in the highest pier. It is expected that the proposed Bayesian damage identification methodology will promote $M^{[10]}$, $M^{[10,i]}$ and $M^{[5-par]}$ as the most probable model classes since these models classes monitor the stiffness of the component that contains the actual damage.

The model class selection and the model updating is performed using the stochastic simulation algorithm TMCMC with the following settings of the TMCMC parameters: tolCov = 1.0, $\beta = 0.2$ and 1000 samples per TMCMC stage [18]. The results for the log evidence for representative model classes and the corresponding magnitude of damages $\Delta\underline{\theta}_i$ predicted by each model class are reported in Table 4 for the two cases of reduced-order models. Herein, for demonstration purposes, the percentage change $\Delta\underline{\theta}_i$ between the mean estimates $\overline{\underline{\theta}}^{[i]}$ (or $\overline{\underline{\theta}}^{[i,j]}$, $\overline{\underline{\theta}}^{[5-par]}$) of the model parameters of each model class and the corresponding values $\hat{\underline{\theta}}^{[i,und]}$ (or $\hat{\underline{\theta}}^{[i,j,und]}$, $\hat{\underline{\theta}}^{[5-par,und]}$) of the reference (undamaged) structure measures the severity (magnitude) of damage computed by each model class $M^{[i]}$ (or $M^{[i,j]}$, $M^{[5-par]}$).

Comparing the log evidence of each model class and also the corresponding magnitude of damages $\Delta\underline{\theta}_i$ predicted by each model class in Table 4 it is evident that the proposed methodology correctly predicts the location and magnitude of damage using the reduced-order model classes. Specifically, based on the reduced-order models for $\rho = 8$, the most probable model class is $M^{[10]}$ which predicts a mean 29.2% reduction in stiffness which is very close to the inflicted 30%. Among all alternative model classes $M^{[10]}$, $M^{[10,7]}$, $M^{[10,8]}$ and $M^{[5-par]}$ that contain the actual damage, the proposed methodology favors the model class $M^{[10]}$ with the least number of parameters and it predicts the five parameter model class $M^{[5-par]}$ as the least probable model. This is consistent with theoretical results for model class penalization for over parameterization, available for Bayesian model class selection [14]. The model classes that do not contain the damage are not favored by the proposed methodology. Based on the reduced-order models for $\rho = 8$ and $v = 200$, the predictions of the location and severity of damage are very close to the ones obtained from the reduced-order models for $\rho = 8$ for most model classes included in Table 4. In particular, the most probable model class for $\rho = 8$ and $v = 200$ is also predicted to be $M^{[10]}$, while the mean damage severity is predicted to correspond to 29.2% reduction in stiffness, exactly the same as the one predicted with the reduced-order models for $\rho = 8$.

The resulting number of FE model re-analyses and the computational demands in minutes for each model class are also is shown in Table 4. The number of FE model runs for each model class depends on the number of TMCMC stages which vary for each model class from 8 for the one-parameter model class to 19 for the five-parameter model class. The resulting variable number of stages per model class was automatically obtained from the TMCMC algorithm by keeping constant the value tolCov of the TMCMC parameter to tolCov = 1.0. This parameter controls the intermediate PDFs. For more details, the reader is referred to the original publication of the TMCMC algorithm [18]. The parallelization features of TMCMC [51] were also exploited, taking advantage of the available four-core multi-threaded computer unit to simultaneously run eight TMCMC samples in parallel. For comparison purposes, the computational effort for solving the eigenvalue problem of the original unreduced FE model is approximately 139 s. Multiplying this by the number of TMCMC samples shown in Table 4 and considering parallel implementation in a four-core multi-threaded computer unit, the total computational effort for each model class is expected to be of the order of 3 to 7 days for 8000 to 19,000 samples, respectively. The results from the full FE model are not shown due to the excessive computational time required to obtain results for the model classes in the database. For all eight model classes considered in Table 4, the total computational effort using the unreduced models is estimated to be approximately one month and seven days. In contrast, for the reduced-order models for $\rho = 8$, the computational demands for running all model classes are reduced to 30 h (2155 min as shown in the last row of Table 4), while for the reduced-order models for $\rho = 8$ and $v = 200$ these computational demands are drastically reduced to 40 min. It is thus evident that a drastic reduction in computational effort for performing the structural identification based on a set of monitoring data is achieved from approximately 37 days for the unreduced model classes to 40 min for the reduced model classes corresponding to $\rho = 8$ and $v = 200$, without compromising the predictive capabilities of the proposed damage identification methodology. This results in a drastic reduction in the computational effort of more than three orders of magnitude.

6. Conclusions

Iterative optimization algorithms and stochastic simulation algorithms involved in both deterministic and Bayesian FE model updating formulations require a moderate to large number of FE model re-analyses. For large size FE models with hundred of thousands or even million DOF, the computational demands may be excessive. Exploiting certain stiffness-related parameterization schemes, often encountered in FE model updating formulations, to guide the division of the structure into components results in exact linear representations of the Craig–Bampton reduced stiffness matrix as a function of the model parameters with coefficient matrices computed and assembled once from a single CMS analysis of a reference structure. Further significant reductions in the size of the reduced system are shown to be possible using characteristic interface modes estimated for each interface between components. Re-analyses required in FE model updating formulations are associated with the solution of the eigenproblem of the reduced-order system, completely avoiding the re-analyses of the component fixed-interface and characteristic interface modes as well as the re-assembling of the reduced system matrices. FE model updating and damage identification results using a solid model of a bridge demonstrated the implementation, computational efficiency and accuracy of the proposed model reduction methodology. The computational effort was reduced drastically by more than three orders of magnitude. In particular, for the application in damage identification the computational time was reduced from approximately one month to several minutes. Further computational savings can be obtained by adopting surrogate modes to drastically reduce the number of reduced-order system re-analyses and parallel computing algorithms to efficiently distribute the computations in available multi-core CPUs [51].

Acknowledgments

This research has been co-financed by the European Union (European Social Fund – ESF) and Greek national funds through the Operational Program "Education and Lifelong Learning" of the National Strategic Reference Framework (NSRF) – Research Funding Program: Heracleitus II. Investing in knowledge society through the European Social Fund.

References

[1] Yuen KV, Kuok SC. Bayesian methods for updating dynamic models. Appl Mech Rev 2011;64(1).

[2] Mottershead JE, Friswell MI. Model updating in structural dynamics: a survey. J Sound Vib 1993;167:347–75.
[3] Marwala T. Finite element model updating using computational intelligence techniques: applications to structural dynamics. Springer; 2010.
[4] Moaveni B, He X, Conte JP, De Callafon RA. Damage identification of a composite beam using finite element model updating. Comput Aided Civil Infrastruct Eng 2008;23(5):339–59.
[5] Christodoulou K, Papadimitriou C. Structural identification based on optimally weighted modal residuals. Mech Syst Signal Process 2007;21:4–23.
[6] Katafygiotis LS, Papadimitriou C, Lam HF. A probabilistic approach to structural model updating. Int J Soil Dynam Earthquake Eng 1998;17:495–507.
[7] Fritzen CP, Jennewein D, Kiefer T. Damage detection based on model updating methods. Mech Syst Signal Process 1998;12(1):163–86.
[8] Yuen K-V, Beck JL, Katafygiotis LS. Efficient model updating and health monitoring methodology using incomplete modal data without mode matching. Struct Control Health Monit 2006;13:91–107.
[9] Haralampidis Y, Papadimitriou C, Pavlidou M. Multi-objective framework for structural model identification. Earthquake Eng Struct Dynam 2005;34(6): 665–85.
[10] Christodoulou K, Ntotsios E, Papadimitriou C, Panetsos P. Structural model updating and prediction variability using Pareto optimal models. Comput Methods Appl Mech Eng 2008;198(1):138–49.
[11] Das I, Dennis Jr JE. Normal-boundary intersection: a new method for generating the Pareto surface in nonlinear multi-criteria optimization problems. SIAM J Optim 1998;8:631–57.
[12] Beck JL, Katafygiotis LS. Updating models and their uncertainties – I: Bayesian statistical framework. ASCE J Eng Mech 1998;124(4):455–61.
[13] Yuen K-V. Bayesian methods for structural dynamics and civil engineering. John Wiley & Sons; 2010.
[14] Beck JL, Yuen KV. Model selection using response measurements: Bayesian probabilistic approach. ASCE J Eng Mech 2004;130(2):192–203.
[15] Yuen KV. Recent developments of Bayesian model class selection and applications in civil engineering. Struct Safety 2010;32(5):338–46.
[16] Papadimitriou C, Beck JL, Katafygiotis LS. Updating robust reliability using structural test data. Probab Eng Mech 2001;16:103–13.
[17] Metropolis N, Rosenbluth AW, Rosenbluth MN, Teller AH, Teller E. Equation of state calculations by fast computing machines. J Chem Phys 1953;21(6): 1087–92.
[18] Ching J, Chen YC. Transitional Markov Chain Monte Carlo method for Bayesian updating, model class selection, and model averaging. ASCE J Eng Mech 2007;133:816–32.
[19] Haario H, Laine M, Mira A, Saksman E. DRAM: efficient adaptive MCMC. Stat Comput 2006;16:339–54.
[20] Beck JL, Au SK. Bayesian updating of structural models and reliability using Markov chain Monte Carlo simulation. ASCE J Eng Mech 2002;128(4):380–91.
[21] Vanik MW, Beck JL, Au SK. Bayesian probabilistic approach to structural health monitoring. ASCE J Eng Mech 2000;126:738–45.
[22] Ntotsios E, Papadimitriou C, Panetsos P, Karaiskos G, Perros K, Perdikaris Ph. Bridge health monitoring system based on vibration measurements. Bull Earthquake Eng 2009;7(2):469–83.
[23] Teughels A, De Roeck G. Damage detection and parameter identification by finite element model updating. Arch Comput Methods Eng 2005;12(2): 123–64.
[24] Yuen K-V, Au SK, Beck JL. Structural damage detection and assessment using adaptive Markov Chain Monte Carlo simulation. J Struct Control Health Monit 2004;11:327–47.
[25] Friswell MI, Mottershead JE. Inverse methods in structural health monitoring. Key Eng Mater 2001;204–05:201–10.
[26] Moaveni B, He X, Conte JP, Restrepo JI. Damage identification study of a seven-story full-scale building slice tested on the UCSD-NEES shake table. Struct Safety 2010;32(5):347–56.
[27] Fan W, Qiao P. Vibration-based damage identification methods: a review and comparative study. Struct Health Monit 2011;10(1):83–111.
[28] Lopez I, Sarigul-Klijn N. A review of uncertainty in flight vehicle structural damage monitoring, diagnosis and control: challenges and opportunities. Prog Aerosp Sci 2010;46(7):247–73.
[29] Yuen KV, Beck JL. Reliability-based robust control for uncertain dynamical systems using feedback of incomplete noisy response measurements. Earthquake Eng Struct Dynam 2003;32(5):751–70.
[30] Craig Jr RR, Bampton MCC. Coupling of substructures for dynamic analysis. AIAA J 1965;6(7):678–85.
[31] Craig Jr RR. Structural dynamics –an introduction to computer methods. New York: John Wiley & Sons; 1981.
[32] Hurty W. Dynamic analysis of structural systems using component modes. AIAA J 1965;3(4):678–85.
[33] Balmes E. Parametric families of reduced finite element models. Theory and applications. Mech Syst Signal Process 1996;10(4):381–94.
[34] Pradlwarter H, Schueller G, Szıkely G. Random eigenvalue problems for large systems. Comput Struct 2002;80:2415–24.
[35] Hinke L, Dohnal F, Mace B, Waters T, Ferguson N. Component mode synthesis as a framework for uncertainty analysis. J Sound Vib 2009;324(1–2): 161–78.
[36] Mace B, Shorter P. A local modal/perturbational method for estimating frequency response statistics of built-up structures with uncertain properties. J Sound Vib 2001;242(5):793–811.
[37] Goller B, Pradlwarter HJ, Schueller GI. An interpolation scheme for the approximation of dynamical systems. Comput Methods Appl Mech Eng 2011;200:414–23.
[38] Goller B, Broggi M, Calvi A, Schueller GI. A stochastic model updating technique for complex aerospace structures. Finite Elem Anal Des 2011;47: 739–52.
[39] Goller B. Stochastic model validation of structural systems. Ph.D. Dissertation, University of Innsbruck; 2011.
[40] Hong S-K, Epureanu BI, Castanier MP, Gorsich DJ. Parametric reduced-order models for predicting the vibration response of complex structures with component damage and uncertainties. J Sound Vib 2011;330:1091–110.
[41] Papadimitriou C, Katafygiotis LS. Bayesian modeling and updating. In: Nikolaidis N, Ghiocel DM, Singhal S, editors. Engineering design reliability handbook. CRC Press; 2004.
[42] Muto M, Beck JL. Bayesian updating and model class selection using stochastic simulation. J Vib Control 2008;14:7–34.
[43] Nelson RB. Simplified calculation of eigenvector derivatives. AIAA J 1976;14(9):1201–5.
[44] Fox RL, Kapoor MP. Rate of change of eigenvalues and eigenvectors. AIAA J 1968;6(12):2426–9.
[45] Ntotsios E, Papadimitriou C. Multi-objective optimization algorithms for finite element model updating. In: ISMA2008 International Conference on Noise and Vibration Engineering, Leuven; 2008. p. 1895–909.
[46] Teughels A, De Roeck G, Suykens JAK. Global optimization by coupled local minimizers and its application to FE model updating. Comput Struct 2003; 81(24–25):2337–51.
[47] Casciati S. Stiffness identification and damage localization via differential evolution algorithms. Struct Control Health Monit 2008;15:436–49.
[48] Beyer HG. The theory of evolution strategies. Berlin: Springer-Verlag; 2001.
[49] Castanier MP, Tan Y-C, Pierre C. Characteristic constraint modes for component mode synthesis. AIAA J 2001;39(6):1182–7.
[50] COMSOL AB COMSOL Multiphysics User's Guide. 2005 [<http://www.comsol.com/>].
[51] Angelikopoulos P, Papadimitriou C, Koumoutsakos P. Bayesian uncertainty quantification and propagation in molecular dynamics simulations. : A high performance computing framework. J Chem Phys 2012;137(14). http://dx.doi.org/10.1063/1.4757266.